Human Cep192 and Cep152 cooperate in Plk4 recruitment and centriole duplication

Katharina F. Sonnen[1],[*], Anna-Maria Gabryjonczyk[1], Eduard Anselm[1],[‡], York-Dieter Stierhof[2] and Erich A. Nigg[1],[§]

[1]Biozentrum, University of Basel, Klingelbergstrasse 50/70, 4056 Basel, Switzerland
[2]ZMBP, Mikroskopie, Universität Tübingen, Auf der Morgenstelle 5, 72076 Tübingen, Germany

[*]Present address: EMBL, Meyerhofstraße 1, 69117 Heidelberg, Germany
[‡]Present address: Max-Planck Institute of Immunobiology and Epigenetics, Stübeweg 51, 79108 Freiburg, Germany
[§]Author for correspondence (erich.nigg@unibas.ch)

Summary

Polo-like kinase 4 (Plk4) is a key regulator of centriole duplication, but the mechanism underlying its recruitment to mammalian centrioles is not understood. In flies, Plk4 recruitment depends on Asterless, whereas nematodes rely on a distinct protein, Spd-2. Here, we have explored the roles of two homologous mammalian proteins, Cep152 and Cep192, in the centriole recruitment of human Plk4. We demonstrate that Cep192 plays a key role in centrosome recruitment of both Cep152 and Plk4. Double-depletion of Cep192 and Cep152 completely abolishes Plk4 binding to centrioles as well as centriole duplication, indicating that the two proteins cooperate. Most importantly, we show that Cep192 binds Plk4 through an N-terminal extension that is specific to the largest isoform. The Plk4 binding regions of Cep192 and Cep152 (residues 190–240 and 1–46, respectively) are rich in negatively charged amino acids, suggesting that Plk4 localization to centrioles depends on electrostatic interactions with the positively charged polo-box domain. We conclude that cooperation between Cep192 and Cep152 is crucial for centriole recruitment of Plk4 and centriole duplication during the cell cycle.

Key words: Cep152, Cep192, Plk4, Centriole duplication, Centrosome

Introduction

Centrioles are barrel-shaped, microtubule-based structures that are duplicated exactly once in every cell cycle and serve as platforms for the assembly of centrosomes and cilia (Bettencourt-Dias et al., 2011; Bornens, 2012; Gönczy, 2012; Lüders and Stearns, 2007; Nigg and Raff, 2009). Centrosomes constitute the major microtubule-organizing centers of animal cells. Each centrosome comprises two centrioles embedded in a protein matrix known as the pericentriolar material (PCM). During interphase, the centrosome is important for intracellular transport and organelle positioning, as well as for cell shape and motility; during mitosis, the duplicated centrosomes associate with the poles of the bipolar spindle, which in turn is important for chromosome segregation. In quiescent and differentiated cells, centrioles function as basal bodies for the formation of cilia and flagella. Anomalies in centrosome number and/or structure have long been implicated in tumorigenesis (Basto et al., 2008; Ganem et al., 2009; Nigg, 2002). More recently, genetic studies have revealed that mutations in centriolar and centrosomal proteins are responsible for a variety of developmental diseases, notably ciliopathies, microcephaly and dwarfism (Bettencourt-Dias et al., 2011; Davis and Katsanis, 2012; Megraw et al., 2011; Nigg and Raff, 2009; Thornton and Woods, 2009).

Centriole duplication during S phase is initiated by the assembly of a procentriole (termed 'daughter centriole') orthogonally to the proximal base of each pre-existing centriole (termed 'parental' or 'mother centriole'). Pioneering work in *Caenorhabditis elegans* has revealed a pathway for centriole biogenesis in which the coiled-coil protein Spd-2 is required for the recruitment of a kinase, Zyg-1, to the mother centriole (Kemp et al., 2004; O'Connell et al., 2001; O'Connell et al., 2000; Pelletier et al., 2004). This kinase then induces the recruitment of two structural proteins, Sas-6 and Sas-5, and these in turn mediate the recruitment of a third protein, Sas-4, which triggers the assembly of procentriolar microtubules (Delattre et al., 2006; Kirkham et al., 2003; Leidel et al., 2005; Leidel and Gönczy, 2003; Pelletier et al., 2006). This assembly pathway was corroborated by cryoelectron tomography showing that *C. elegans* Sas-6 forms a central tube around which the MTs of the new centriole are assembled in a Sas-4-dependent manner (Pelletier et al., 2006). Most recently, X-ray crystallography and electron microscopy were combined to demonstrate that Sas-6 can self-assemble into a cartwheel-like structure, indicating that Sas-6 plays a key role in conferring the typical 9-fold symmetry to centrioles (Guichard et al., 2012; Kitagawa et al., 2011; van Breugel et al., 2011). Extensive work on centriole assembly was also conducted in other species, notably *Drosophila* and vertebrates (e.g. Dobbelaere et al., 2008; Kleylein-Sohn et al., 2007). Collectively, these studies demonstrate that centriole assembly is governed by an evolutionarily conserved mechanism that relies on structural and/or functional homologs of the described *C. elegans* gene products (Carvalho-Santos et al., 2010; Strnad and Gönczy, 2008).

A serine/threonine kinase of the Polo family is central to centriole duplication in all species examined. This kinase is known as Zyg-1 in *C. elegans* and as Polo-like kinase 4 (Plk4) or

Sak in *D. melanogaster* and vertebrates (Bettencourt-Dias et al., 2005; Habedanck et al., 2005). In both human cells and *Drosophila*, depletion of Plk4/Sak causes the progressive loss of centrioles in successive cell divisions. Conversely, overexpression of Plk4/Sak leads to centriole amplification (Bettencourt-Dias et al., 2005; Habedanck et al., 2005; Kleylein-Sohn et al., 2007), and expression of Plk4/Sak is sufficient to trigger *de novo* centriole formation in *Drosophila* eggs (Rodrigues-Martins et al., 2007). A few substrates of Zyg-1 or Plk4/Sak have recently been identified, including Sas-6 (in *C. elegans*; Kitagawa et al., 2009), Cep152 (Hatch et al., 2010), Fbxw5 (Puklowski et al., 2011), CPAP/hSas-4 (Chang et al., 2010) and GCP6 (Bahtz et al., 2012), but the functional consequences of these phosphorylations remain to be fully understood. Likewise, to better understand the mechanism underlying centriole biogenesis it will be important to elucidate the regulation of the Zyg-1/Plk4/Sak family. In human cells, for example, excess Plk4 triggers the near-simultaneous formation of multiple centrosomes, suggesting that the local concentration of Plk4 at centrosomes is critical for controlling the number of nascent centrioles (copy number control) (Nigg, 2007). Hence, it will be crucial to understand the mechanisms that control the expression and localization of Plk4. In both human cells and *Drosophila*, the levels of Plk4/Sak are regulated by trans-auto-phosphorylation that leads to βTrCP- and proteasome-dependent degradation (Cunha-Ferreira et al., 2009; Guderian et al., 2010; Holland et al., 2012; Holland et al., 2010; Rogers et al., 2009; Sillibourne et al., 2010). Furthermore, phosphatase 2A has been implicated in regulating the stability of Plk4/Sak in flies and Zyg-1 in worms (Brownlee et al., 2011; Song et al., 2011). In contrast, it is not yet well understood how mammalian Plk4/Sak is targeted to centrosomes. Centrosome localization clearly depends on the C-terminal (non-catalytic) domain (Fode et al., 1994; Habedanck et al., 2005), which comprises three so-called polo-boxes (Slevin et al., 2012), but the identity of the centrosomal interaction partner(s) of mammalian Plk4/Sak remains to be established.

In the present study, we have explored the mechanism underlying the recruitment of Plk4 to human centrosomes. Specifically, we focused on the role of Cep192 and Cep152. These two large centrosomal proteins are the putative homologs of *C. elegans* Spd-2 and *D. melanogaster* Asterless, respectively. *C. elegans* Spd-2 has been implicated in both PCM assembly and the centrosomal recruitment of Zyg-1 (Kemp et al., 2004; Pelletier et al., 2004), but the *Drosophila* homolog of Spd-2 was reported to function only in PCM assembly (Dix and Raff, 2007). Instead, a role for recruitment of *Drosophila* Plk4/Sak was attributed to Asterless (Dzhindzhev et al., 2010). The *asterless* gene product had originally been identified in a screen for mutants that result in male infertility (Bonaccorsi et al., 1998) and was subsequently shown to function in both PCM recruitment and centriole duplication (Blachon et al., 2008; Varmark et al., 2007). Taken at face value, the above studies on invertebrate species thus suggest that Zyg-1 and Plk4/Sak are recruited to centrosomes through distinct mechanisms. Compounding this uncertainty, conflicting data have been reported for the roles of the vertebrate homologs of Asterless and Spd-2. Cep152, the human homolog of Asterless, was found to interact with Plk4 and be required for centriole duplication, but its contribution to the centrosome recruitment of Plk4 remains controversial (Cizmecioglu et al., 2010; Dzhindzhev et al., 2010;

Hatch et al., 2010). Likewise, two studies describe a requirement for Cep192, the human homolog of Spd-2, in PCM recruitment, but they report conflicting data on the role of this protein in centriole duplication (Gomez-Ferreria et al., 2007; Zhu et al., 2008). A possible contribution of Cep192 to the centrosome recruitment of human Plk4 has not previously been explored.

Results

Expression and localization of Cep152 and Cep192 isoforms

Examination of Ensembl, UniProt and NCBI databases suggests the existence of at least four isoforms for both Cep152 (supplementary material Fig. S1A) and Cep192 (supplementary material Fig. S2A). These isoforms will be referred to as Cep152-1 to Cep152-4 and Cep192-1 to Cep192-4. Cep152-1 and -2 differ from -3 and -4 mainly by the presence of an extended C terminus. As shown by use of antibodies against the N- (Cep152-N) or extended C-terminus (Cep152-C) (supplementary material Fig. S1B,C) (Sonnen et al., 2012), both long (Cep152-1/2) and short (Cep152-3/-4) isoforms are expressed in all human cell lines analyzed here (supplementary material Fig. S1D; Fig. S3B). In the case of human Cep192, an anti-Cep192 antibody recognizing all potential isoforms (Schmidt et al., 2009) showed prominent and specific reactivity towards a band migrating above 250 kDa, suggesting that Cep192-1 represents the prominent species in the human cell lines analyzed here (supplementary material Fig. S2B). This notion was confirmed by the co-migration of endogenous Cep192 with overexpressed FLAG-tagged Cep192-1 (data not shown). We emphasize that Cep192-1 is the predominant isoform expressed in all human cell lines analyzed here, but note that previous studies generally focused on the shorter, N-terminally truncated isoform of Cep192 (Cep192-2) (Gomez-Ferreria et al., 2012; Gomez-Ferreria et al., 2007).

As a first step towards dissecting the functions of Cep152 and Cep192, we compared the precise localization of the two proteins at centrosomes. Using antibodies against the N- or C-termini of Cep152 for immunoelectron microscopy (immuno-EM), we found that Cep152 was confined to the proximal halves of mother centrioles (Fig. 1A, upper and middle panels), in line with previous data (Cizmecioglu et al., 2010; Lukinavičius et al., 2013; Sir et al., 2011). Both antibodies produced indistinguishable staining patterns, suggesting that the centrosomal localizations of long and short Cep152 isoforms are similar. In contrast to Cep152, anti-Cep192 antibodies consistently showed labeling along the entire walls of both mother and daughter centrioles (Fig. 1A, lower panel), indicating that Cep192 shows a broader distribution than Cep152. This conclusion was corroborated by results from 3D-structured illumination microscopy (3D-SIM). Whereas anti-Cep152 antibodies only stained the proximal ends of mother centrioles, antibodies against Cep192 and glutamylated tubulin (GT335) labeled both mother and daughter centrioles along their entire lengths (Fig. 1B).

Cell cycle analysis showed that Cep152 was associated predominantly with the mature (Cep164-positive) mother centriole during G1 phase but recruited to the second parental centrioles during centriole duplication (supplementary material Fig. S3A). Overall levels of Cep152 increased after release from a thymidine arrest (supplementary material Fig. S3B), (Cizmecioglu et al., 2010), whereas Cep192 levels showed only minor variations during cell cycle progression (supplementary
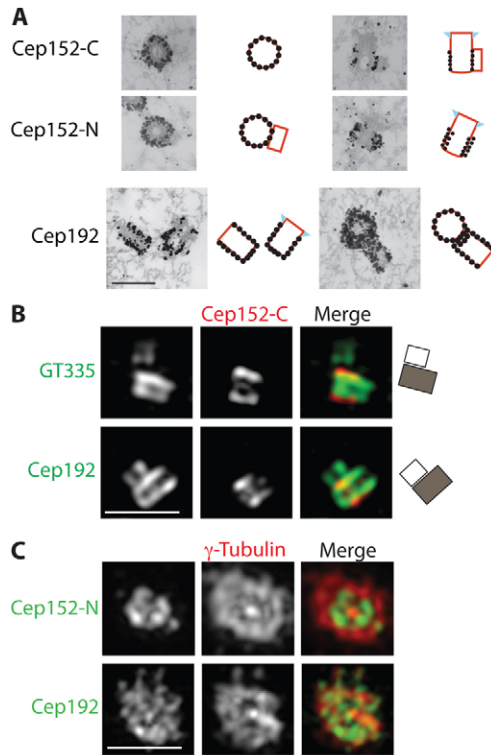
Fig. 1. Cep152 and Cep192 show distinct cell cycle-specific centrosome localizations. (**A**) U2OS cells were fixed and stained for immuno-EM using antibodies against the N- or C-terminal domains of Cep152 or antibodies against Cep192, followed by nanogold-labeled secondary antibodies. (**B,C**) U2OS cells were fixed and stained for 3D-SIM with the indicated antibodies. Interphase (B) and mitotic cells (C) were distinguished by the distance between the centriole pairs. Centriole orientation is illustrated schematically. Scale bars: 1 µm.

material Fig. S3B). Throughout mitosis, both Cep152 and Cep192 localized to the poles of the mitotic spindle (supplementary material Fig. S3C,D). However, whereas Cep152 remained confined to the proximity of centrioles, Cep192 spread throughout the expanding PCM of mitotic cells (Fig. 1C). As in the case of the Cep152 isoforms, no significant differences could be seen when comparing the localizations of Cep192 isoforms: after transfection of FLAG-tagged Cep192-1 and Cep192-2, both proteins localized close to centrioles during interphase but spread throughout the expanding PCM during mitosis (supplementary material Fig. S3E). Furthermore, analysis of the localizations of FLAG-tagged Cep192-1 and Cep192-2 by 3D-SIM revealed no significant differences between the two isoforms (data not shown).

Centrosome localization of Cep152 depends on Cep192
Next, we investigated a possible interdependence between Cep152 and Cep192 for centrosome localization. Whereas siRNA-mediated depletion of Cep152 did not detectably affect Cep192 localization, depletion of Cep192 led to a strong, albeit not complete loss of centrosomal Cep152 (Fig. 2A,B). Localization of Cep135, analyzed for control, was not affected upon depletion of either Cep152 or Cep192 (Fig. 2A,B). As demonstrated by western blotting, the effect of Cep192 depletion on Cep152 localization could not be attributed to changes in cellular protein levels (Fig. 2C). Furthermore, depletion of

another PCM component, Pericentrin, did not detectably interfere with localization of either Cep192 (Fig. 2D) or Cep152 (Fig. 2E). Collectively, these results indicate that the association of Cep152 with centrosomes depends on Cep192 but not vice versa. Consistent with recent reports (Cizmecioglu et al., 2010; Dzhindzhev et al., 2010; Lukinavičius et al., 2013; Sir et al., 2011), the centrosome localization of both Cep63 and CPAP was dependent on Cep152 (Fig. 2F; supplementary material Fig. S4; data not shown for CPAP). Furthermore, centrosomal levels of Cep63 and CPAP were also reduced upon depletion of Cep192, in line with the dependency of Cep152 localization on Cep192 (Fig. 2F; supplementary material Fig. S4). Conversely, depletion of CPAP did not detectably affect the centrosomal levels of any of the proteins analyzed here (other than CPAP itself), and Cep135, hSas-6 and CP110 were all resistant to the various depletion regimes (data not shown; summarized in Fig. 2F).

To explore possible interactions between Cep192, Cep152, Cep63 and CPAP, we next carried out co-immunoprecipitation experiments. Cep192 could readily be co-immunoprecipitated with Cep152, but not with Cep63 or CPAP (Fig. 3A). Interestingly, Cep152 was brought down with both Cep192-1 and Cep192-2, but not with the N-terminus of Cep192-1 (residues 1–519), indicating that the N-terminus of Cep192-1 is dispensable for the interaction with Cep152 (Fig. 3B,D). Conversely, the central coiled-coil region of Cep152 (amino acids 221–1308) was both necessary and sufficient for the interaction with Cep192-1 (Fig. 3C,D).

Cep192 and Cep152 cooperate in Plk4 recruitment
Whereas Spd-2 was identified as a centrosomal recruitment factor for Zyg-1 in *C. elegans* (O'Connell et al., 2001), a corresponding role for the recruitment of Plk4/Sak has been attributed to the product of the *asterless* gene in *Drosophila* (Dzhindzhev et al., 2010). Hence, we asked to what extent Cep192 and/or Cep152, the respective vertebrate homologs of *C. elegans* Spd-2 and *Drosophila* Asterless, might contribute to the centrosome recruitment of human Plk4. Depletion of Cep152 from U2OS cells did not significantly interfere with Plk4 recruitment to centrioles; instead we observed a slight increase in centrosomal Plk4 staining (Fig. 4A,B), in line with earlier reports (Cizmecioglu et al., 2010; Dzhindzhev et al., 2010; Hatch et al., 2010). In striking contrast, depletion of Cep192 strongly reduced the centrosomal levels of Plk4, and co-depletion of Cep192 and Cep152 completely prevented Plk4 association with centrosomes (Fig. 4A,B). Depletion of Pericentrin, analyzed for control, had no significant effect (supplementary material Fig. S5A; Fig. 4B). Western blotting showed that these results reflect impaired localization and not merely reductions in overall Plk4 protein levels (data not shown).

Cep152 has previously been described to be required for centrosome association of newly synthesized Plk4 (Cizmecioglu et al., 2010). Thus, we also examined the effects of depleting Cep152 and/or Cep192 on the recruitment of myc-tagged Plk4 expressed from an inducible promoter. Myc-Plk4 expression showed considerable variation amongst individual cells, making rigorous quantification of this experiment impossible. In spite of this caveat, our results clearly show that Plk4 recruitment could be completely abolished only by co-depletion of Cep152 and Cep192, but not by single depletion of these proteins (supplementary material Fig. S5B). These results are in excellent agreement with our data on endogenous Plk4 and allow us to
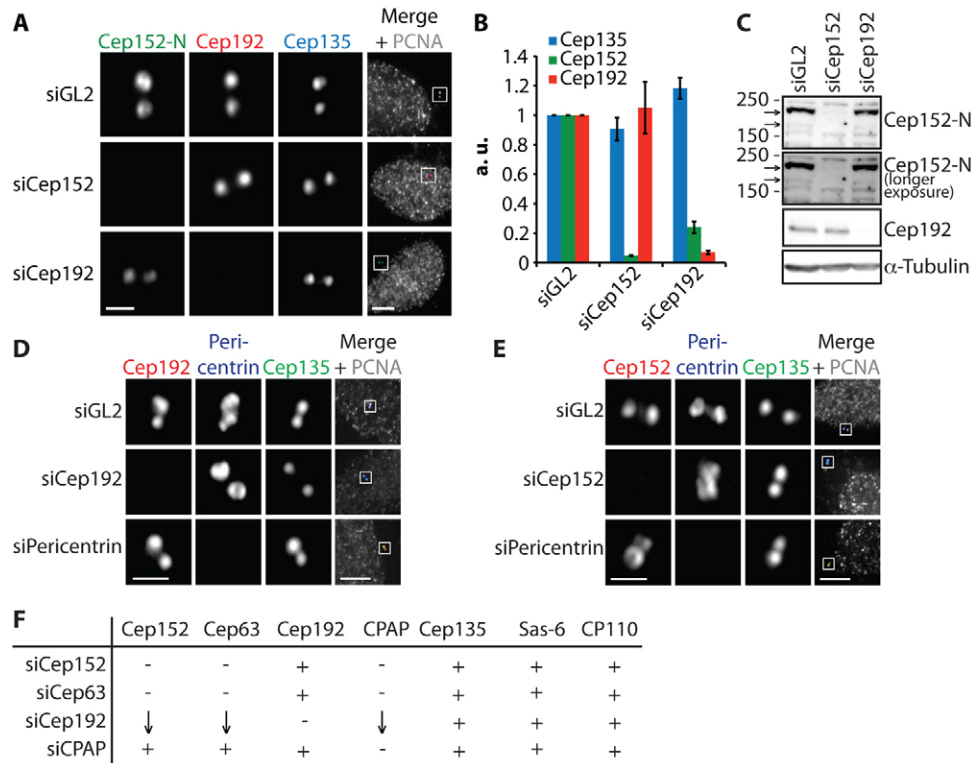
Fig. 2. Cep192 is important for centrosome recruitment of Cep152. (**A,B**) U2OS cells were transfected with the indicated siRNA oligonucleotides for 72 hours before they were fixed and stained with the indicated antibodies. Anti-PCNA was used to visualize S phase cells. (**A**) Representative images. (**B**) Quantification of centrosomal Cep135, Cep192 and Cep152 levels (three independent experiments, 10 cells each; error bars indicate s.e.m.). (**C**) Whole cell lysates were analyzed by western blotting using the indicated antibodies. (**D,E**) U2OS cells were transfected with the indicated siRNA oligonucleotides for 72 hours before they were fixed and stained with the indicated antibodies. Anti-PCNA was used to identify S phase cells. (**F**) Table summarizing all interdependencies for centrosome localizations, as determined by siRNA and immunofluorescence microscopy (exemplified in A,D,E). +, no detectable reduction of centrosomal protein; −, near-complete loss from centrosome; arrow, partial reduction of centrosomal protein. Scale bars: 1 μm (5 μm in overview images, right panels).
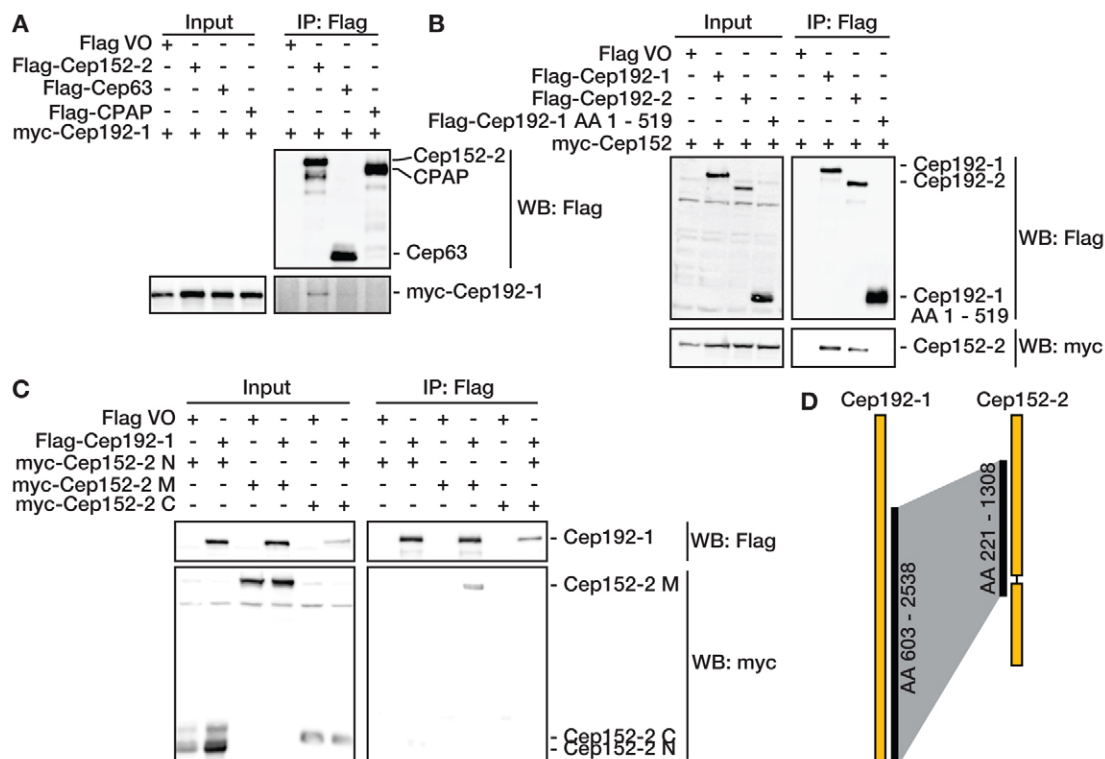

Fig. 3. Interaction of Cep152 and Cep192. (**A–C**) HEK293T cells were transfected with the indicated plasmids for 18 hours. After lysis, anti-FLAG immunoprecipitations were performed and analyzed by western blotting using the indicated antibodies. (**D**) Scheme of identified interaction domains.
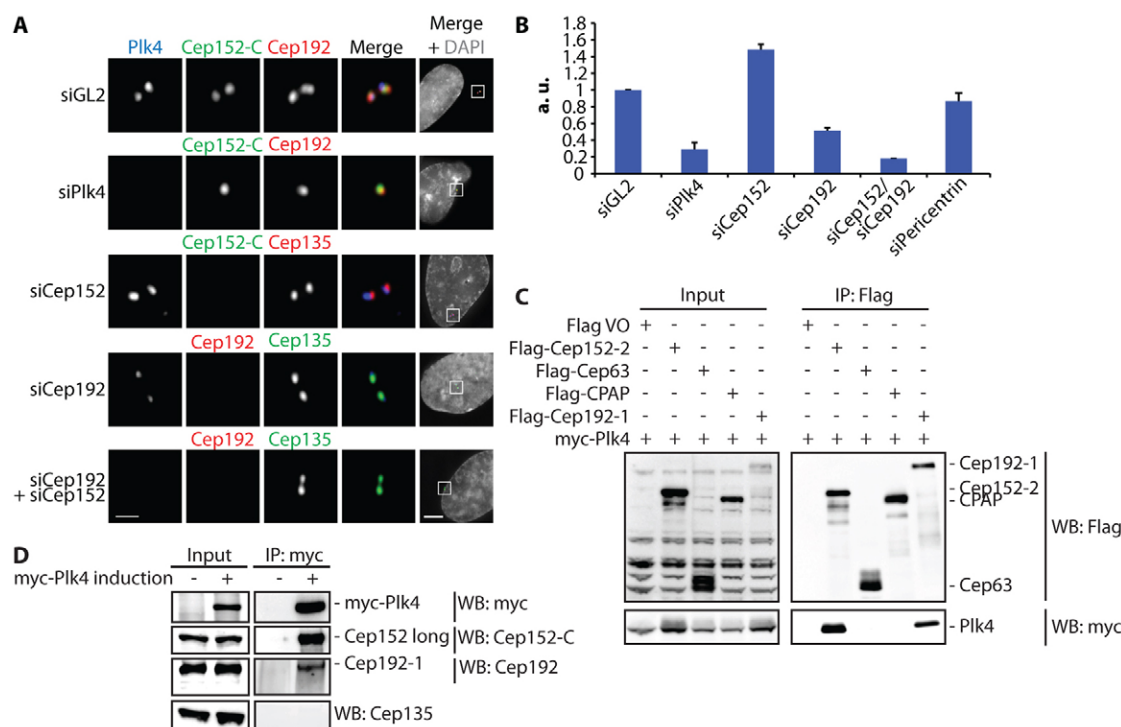
Fig. 4. **Cep192 and Cep152 cooperate in the centrosome recruitment of Plk4.** (**A,B**) U2OS cells were transfected with the indicated siRNA oligonucleotides for 72 hours. After fixation, the cells were stained with the indicated antibodies and DNA was stained with DAPI. (A) Representative images. (B) Quantification of centrosomal Plk4 levels (three independent experiments, 10–15 cells each; error bars indicate s.e.m.). For immunofluorescence data on Pericentrin siRNA see supplementary material Fig. S5A. (**C**) HEK293T cells were transfected with the indicated plasmids. After lysis, anti-FLAG immunoprecipitations were performed and analyzed by western blotting using the indicated antibodies. (**D**) Myc-Plk4 expression was induced in U2OS:myc-Plk4 cells for 16 hours. After lysis, anti-myc immunoprecipitations were performed and analyzed by western blotting using the indicated antibodies. Scale bars: 1 µm (5 µm in overview images, right panels).

conclude that Cep192 and Cep152 cooperate in the recruitment of Plk4 to human centrosomes.

Previous studies had focused on the characterization of Cep152 as a prominent interaction partner of Plk4 (Cizmecioglu et al., 2010; Dzhindzhev et al., 2010; Hatch et al., 2010). Having observed that Cep192 is more critical for centrosome recruitment of Plk4 than Cep152, we next asked whether Cep192 might also interact with Plk4. Indeed, myc-Plk4 could be co-immunoprecipitated after co-expression with either FLAG-Cep192-1 or FLAG-Cep152-2 (Fig. 4C). In contrast, myc-Plk4 did not co-precipitate with FLAG-CPAP or FLAG-Cep63 (Fig. 4C). Co-precipitation of endogenous Plk4 could not be visualized, presumably reflecting the low levels of endogenous Plk4 (data not shown). In converse experiments, we induced expression of myc-Plk4 expression in U2OS cells and, following anti-myc immunoprecipitation, could readily detect endogenous Cep192 as well as Cep152 in the precipitates, whereas Cep135, analyzed for control, was absent (Fig. 4D). These results indicate that both Cep192 and Cep152 interact with Plk4 in human cells.

Interestingly, myc-Plk4 could be co-immunoprecipitated with full length Cep192-1 but not Cep192-2, indicating that the N-terminus specific to the Cep192-1 isoform is required for this interaction (Fig. 5A). In support of this view, the N-terminus alone (residues 1–519 of Cep192-1) was sufficient to co-immunoprecipitate myc-Plk4 (Fig. 5A). Conversely, Plk4 was found to interact with Cep192-1 through a region formerly referred to as 'cryptic polo box' but now recognized to comprise

two of three polo boxes (Slevin et al., 2012) (Fig. 5B; residues 570–820). This region is also sufficient for the interaction with Cep152-2 (Fig. 5B), (Dzhindzhev et al., 2010; Cizmecioglu et al., 2010; Hatch et al., 2010). Furthermore, a fraction, albeit small, of a bacterially expressed recombinant fragment of Cep192-1 (1–330) consistently bound to GST-tagged Plk4 (residues 570–820) (Fig. 5C), supporting a direct interaction between the two proteins. Further narrowing of the Plk4-binding domain within Cep192-1 identified the region spanning residues 190–240 of Cep192-1 as being sufficient for the interaction (Fig. 5D). When expressed *in vivo*, this minimal Plk4-binding N-terminal fragment of Cep192-1 did not localize to centrosomes but instead sequestered Plk4 away from centrosomes (Fig. 5E). A similar sequestration phenotype was also seen when expressing the N-terminus of Cep152-2 (1–46) in U2OS cells (Fig. 5E), confirming and extending previous data on the importance of this region for Plk4 binding (Cizmecioglu et al., 2010; Dzhindzhev et al., 2010; Hatch et al., 2010). Interestingly, the regions identified here as being important for binding to Plk4 in both Cep192 (residues 190–240) and Cep152 (residues 1–46; supplementary material Fig. S6A) comprise evolutionarily conserved stretches of acidic residues (supplementary material Fig. S6B,C), suggesting that the binding of Plk4 to centrosomal docking proteins is mediated through electrostatic interactions.

Collectively, these results demonstrate that the extended N-terminus of Cep192-1 is both necessary and sufficient for the interaction of Cep192 with Plk4. They also imply that the shorter
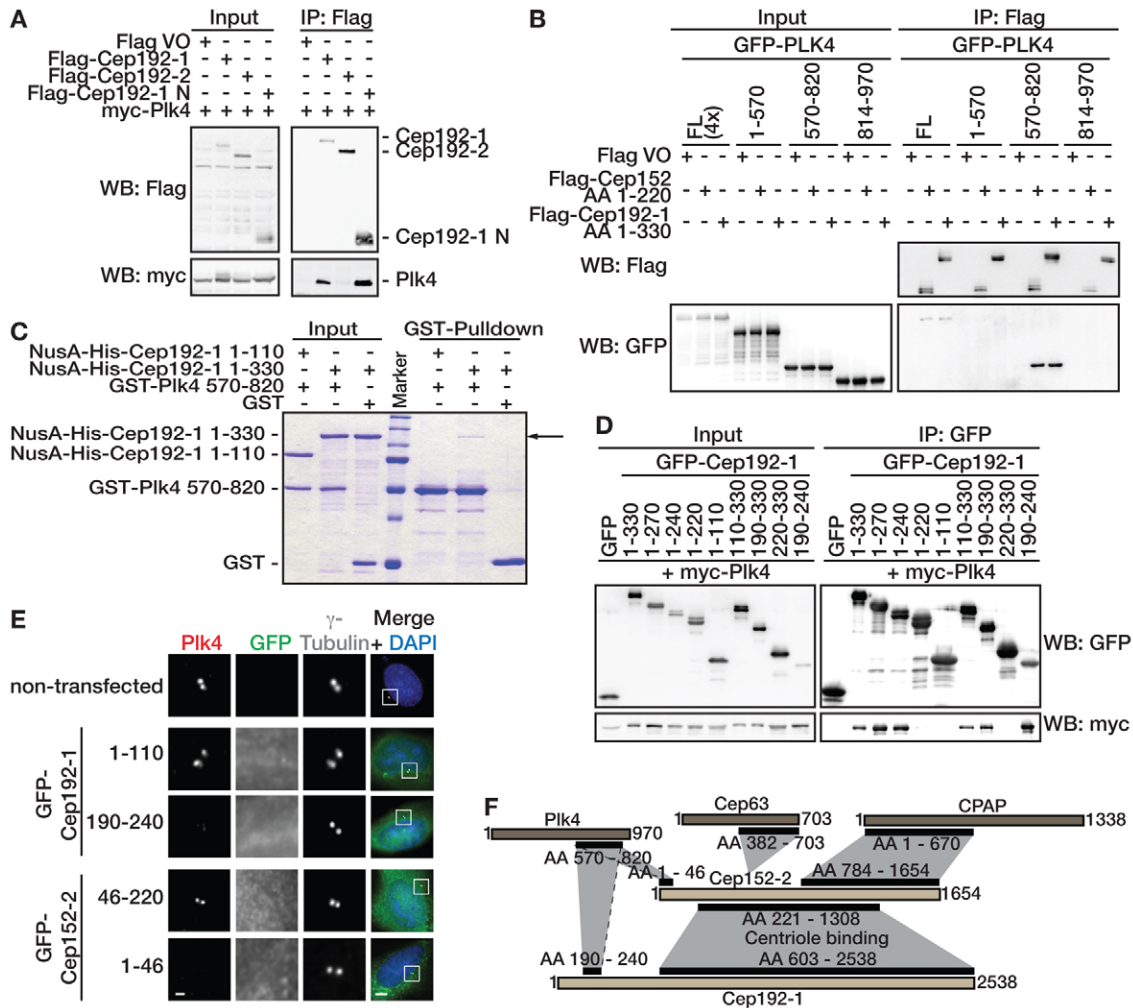
Fig. 5. The N-terminus of Cep192 is important for centrosome recruitment of Plk4. (**A,B**) The indicated plasmids were expressed in HEK293T cells for 18 hours. After lysis, anti-FLAG immunoprecipitations were performed and analyzed by western blotting using the indicated antibodies. (B) Due to low expression levels of GFP-Plk4 full length (FL), these samples were loaded with four times more volume (4×) on the input gel than the other GFP-Plk4 samples. (**C**) The indicated GST- or NusA-His-tagged constructs were purified from bacteria and subjected to a GST pulldown assay. Proteins were detected by SDS-PAGE and Coomassie Blue staining. The arrow points at the NusA-His-Cep192-1 1–330 fragment that specifically interacts with GST-Plk4 570–820. (**D**) HEK293T cells were transfected with the indicated GFP-Cep192 constructs and myc-Plk4. After lysis, anti-GFP immunoprecipitations were performed and analyzed by western blotting using the indicated antibodies. (**E**) U2OS cells were transfected with the indicated GFP-plasmids. After fixation, the cells were stained with antibodies against Plk4 and γ-tubulin; DNA was stained with DAPI. (**F**) Interaction map involving Cep152 and Cep192. The N-terminal regions of Cep192 (this study) and Cep152 (Hatch et al., 2010; this study) interact with the cryptic polo box of Plk4. Amino acids 603–2538 of Cep192 and the central coiled-coil region of Cep152 are required for mutual interaction and for centriolar localization (this study). Cep152 also interacts with Cep63 (Sir et al., 2011) and CPAP (Cizmecioglu et al., 2010; Dzhindzhev et al., 2010). Scale bars: 1 μm (5 μm in overview images, right panels).

isoform, Cep192-2, which has been investigated in previous studies (Gomez-Ferreria et al., 2012; Gomez-Ferreria et al., 2007), is not competent to interact with Plk4. Fig. 5F summarizes all known interactions between Cep152, Cep192, Cep63, CPAP and Plk4, including domains that are required for centrosome localization.

Cep192 and Cep152 cooperate in centriole duplication

While Cep152 has previously been shown to be important for centriole duplication (Cizmecioglu et al., 2010; Hatch et al., 2010), a role for Cep192 in this process has been controversial (Gomez-Ferreria et al., 2007; Zhu et al., 2008). Our discovery that Cep192 and Cep152 cooperate in the centrosome recruitment of Plk4 led us to predict that these two proteins should also

cooperate in centriole duplication. This prediction was indeed met, as co-depletion of the two proteins resulted in a strong impairment of centriole duplication, both in U2OS cells (Fig. 6A,C) and in U2OS cells overexpressing Plk4 (Fig. 6B,D). Up to 60% of the U2OS cells that had been co-depleted of Cep152 and Cep192 showed at most one centriole (based on the number of CP110 dots per cell), compared to only 35% of cells showing the same phenotype after depletion of either Cep152 or Cep192. Furthermore, the effect of co-depleting Cep192 and Cep152 was almost as severe as that seen after depletion of hSas-6, a genuine centriole duplication factor (70% of cells showing at most one centriole; Fig. 6A,C). Likewise, the centriole overduplication that could be induced by overexpression of Plk4 in U2OS cells was suppressed to a similar extent by depletion of either hSas-6 or
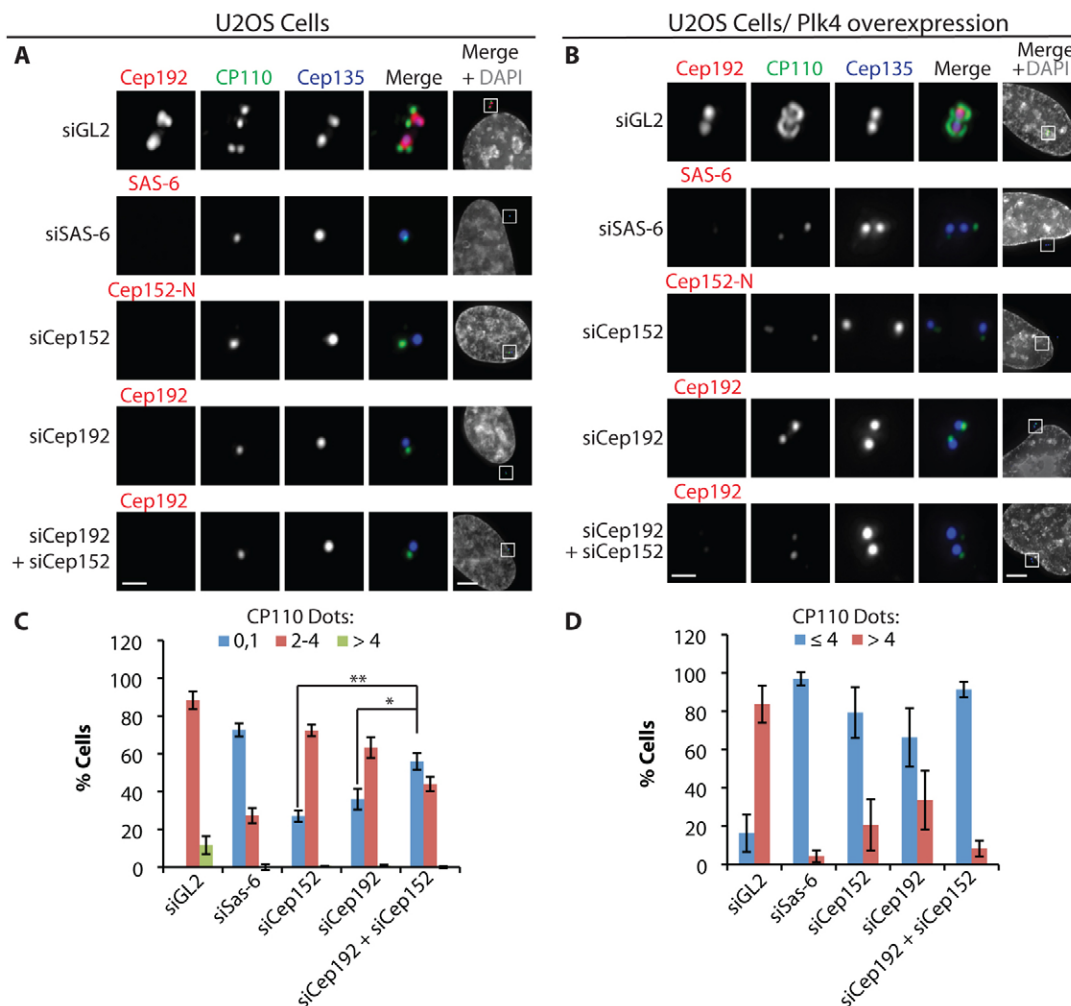
Fig. 6. **Co-depletion of Cep152 and Cep192 abolishes centriole duplication.** (**A**) U2OS were transfected with the indicated siRNA oligonucleotides for 72 hours. After fixation, cells were stained with the indicated antibodies and centriole numbers determined by immunofluorescence microscopy. (**B**) U2OS:myc-Plk4 cells were transfected with the indicated siRNA oligonucleotides for 48 hours. Then, S phase arrest was induced by addition of aphidicolin and 8 hours later myc-Plk4 overexpression was induced for 16 hours by addition of tetracyclin. After fixation, cells were stained with the indicated antibodies and centriole numbers determined by immunofluorescence microscopy. (**C,D**) Quantification of the results shown in A and B, respectively (three independent experiments, 100 cells each; error bars indicate s.e.m.); *$P<0.05$, **$P<0.01$. Scale bars: 1 µm (5 µm in overview images, right panels).

co-depletion of Cep192 and Cep152, but not single depletion of the latter proteins (Fig. 6B,D). Thus, we conclude that Cep192 and Cep152 cooperate in centriole duplication, most likely through their synergism in the centrosome recruitment of Plk4.

Discussion

Here we have investigated the roles of human Cep192 and Cep152 in Plk4 recruitment and centriole duplication. Cep192 and its invertebrate homolog Spd2 have previously been implicated in PCM recruitment and microtubule nucleation (Dix and Raff, 2007; Gomez-Ferreria et al., 2007; Kemp et al., 2004; O'Connell et al., 2000; Pelletier et al., 2004; Zhu et al., 2008). For human Cep192 this function has specifically been attributed to mitotic cells. We now show in addition that Cep192 interacts with Cep152 and that maximal centrosome association of Cep152 in interphase depends on Cep192 but not vice versa. Most importantly, we demonstrate that Cep192-1, the longest isoform of Cep192, directly binds Plk4. This isoform has not

previously been studied, perhaps explaining why the interaction between Cep192 and Plk4 has hitherto escaped detection. As an *in vivo* reflection of this interaction, Cep192 is critical for Plk4 recruitment to centrosomes, whereas a role for Cep152 in Plk4 localization becomes readily apparent only in the absence of Cep192. Co-depletion of both Cep192 and Cep152 then results in complete loss of Plk4 from centrosomes and, concomitantly, impairs centriole duplication. Interestingly, the domains required for Plk4 binding in both Cep192 and Cep152 comprise conserved stretches of acidic residues. Deletion of the acidic domain from Cep192 prevents binding to human Plk4 (this study) and, similarly, deletion of residues 24–55 from *D. melanogaster* Asterless prevents interaction with Sak (Dzhindzhev et al., 2010). Interestingly, *D. melanogaster* Spd-2 is the only one of the analyzed Cep192 family members that lacks the conserved acidic residues and this provides an attractive explanation for why Asterless is indispensable for centriolar recruitment of Sak in flies. Collectively, our data strongly suggest that centriole recruitment of Plk4 depends on electrostatic

interactions between the positively charged polo-box domain (Slevin et al., 2012) and acidic regions within the centrosomal docking proteins Cep192 and Cep152. It will be interesting to see whether direct structural information confirms this prediction.

Cep152 and Cep192 are likely to form multiple complexes

Cep152 has previously been shown to interact with Cep63 and CPAP (Cizmecioglu et al., 2010; Dzhindzhev et al., 2010; Sir et al., 2011). Here we readily confirm these interactions but show in addition that Cep152 also interacts with Cep192. Importantly, Cep152 binds both Cep192-1 and -2, indicating that the N-terminal extension of Cep192-1 is not required for this interaction, although it is required for Plk4 binding by Cep192. Using co-immunoprecipitation experiments we did not detect ternary or quaternary Cep152 complexes comprising both Cep192 and either Cep63 or CPAP. This suggests the existence of distinct Cep152–Cep192 and Cep152–Cep63/CPAP complexes. Similarly, our co-immunoprecipitation experiments did not reveal robust ternary complexes between Cep152–Plk4 and either Cep63 or CPAP, suggesting that Cep152–Plk4 complexes comprise little, if any, CPAP or Cep63. At face value, these results argue for the co-existence of several distinct multiprotein complexes. It is of course possible that co-immunoprecipitation experiments fail to isolate ternary or quaternary complexes because of limited complex stability and/or low abundance of particular components, but we note that the co-existence of multiple distinct complexes is supported by high-resolution immunolocalization data (see below).

Functional cooperation between Cep192 and Cep152

Whereas previous studies on Cep192 have mostly emphasized functions related to PCM expansion and spindle assembly (Dix and Raff, 2007; Gomez-Ferreria et al., 2007; Zhu et al., 2008), our present data also confirm a role for this protein in centriole duplication (Zhu et al., 2008). In particular, we demonstrate that co-depletion of Cep192 and Cep152 results in a centriole duplication phenotype that is nearly as severe as depletion of key duplication factors such as Plk4 or hSas-6. One straightforward interpretation of these findings is that Cep192 and Cep152 cooperate in centriole duplication through their joint role in Plk4 recruitment. This conclusion is supported by phylogenetic expression patterns. Recent studies on the evolution of centrioles in fact suggest that all Plk4-expressing organisms (with the possible exception of *B. dendrobatidis*) express either Cep192 and/or Cep152 (Azimzadeh et al., 2012; Carvalho-Santos et al., 2011). In humans, mutations in the Cep152 gene have recently been identified in patients afflicted by microcephaly and Seckel syndrome (Guernsey et al., 2010; Kalay et al., 2011). Based on the functional relationship between Cep152 and Cep192 in centriole duplication, it will be interesting to determine to what extent mutations in Cep192 may similarly affect mammalian development.

Centrosomal docking of Plk4 through electrostatic interactions

In this study we identify Cep192, specifically the longest isoform Cep192-1 (predicted molecular weight of 279 kDa), as a novel centrosomal docking partner for Plk4. This conclusion is supported by data showing that depletion of Cep192 strongly impairs Plk4 association with centrosomes, whereas, conversely, overexpression of the Plk4-binding domain of Cep192 displaces

Plk4 from the centrosome. Previous studies concur to demonstrate that Cep152, the human homolog of *Drosophila* Asterless, interacts with Plk4 (Cizmecioglu et al., 2010; Dzhindzhev et al., 2010; Hatch et al., 2010). However, whilst Asterless is clearly important for centrosome association of Plk4 in *Drosophila*, partially conflicting results have been reported on a corresponding role for Cep152 in mammalian cells (Cizmecioglu et al., 2010; Dzhindzhev et al., 2010; Hatch et al., 2010). In one study it was suggested that Cep152 is not essential for maintenance of Plk4 at centrosomes but specifically required for centrosome association of newly synthesized Plk4 (Cizmecioglu et al., 2010). In our hands, depletion of Cep152 alone did not impair either Plk4 maintenance at centrosomes or its initial recruitment. However, in the absence of Cep192, the depletion of Cep152 caused a significant additional reduction in centrosomal Plk4 levels. This indicates that the two proteins display partly redundant functions and that Cep152 can partly compensate for the absence of Cep192.

Considering that both Cep192 and Cep152 bind to Plk4, an apparent contradiction arises from our observation that co-depletion of Cep192 and Cep152 affects Plk4 recruitment more severely than single-depletion of either Cep192 or Cep152, and yet single-depletion of Cep192 impairs centrosome association of Cep152. However, we emphasize that depletion of Cep192 does not cause a complete loss of Cep152 from centrosomes, and this residual Cep152 is likely to become important for Plk4 recruitment in the absence of Cep192. Collectively, our data lead us to propose a tentative model according to which, first, Plk4 within cells binds more readily to Cep192 than to Cep152 and, second, a sub-population of Cep152 interacts with Cep192, thereby potentially masking some of the Plk4 interaction sites on Cep192. This model would explain not only why depletion of Cep192 causes a partial loss of centrosomal Cep152, but also why depletion of Cep152 enhances Plk4 binding to centrosomes. For untreated cells, the model would predict that Plk4 recruitment to centrosomes is largely dominated by Cep192, with a minor contribution from Cep152. Upon depletion of Cep152, some Plk4 binding sites would be lost, but this loss would be compensated by the unmasking of additional Plk4 binding sites on Cep192. Conversely, depletion of Cep192 would result in the loss of most Plk4 binding sites on Cep192, along with the population of Cep152 that was bound to Cep192, but it would leave sufficient residual Cep152 to allow for persistence of some Plk4 at centrosomes. Only co-depletion of Cep192 and Cep152 would then completely abolish Plk4 binding.

Evidence for local regulation of Cep192, Cep152 and Plk4 localization

The simple model described above can largely explain the Plk4-related phenotypes that we have observed after siRNA-mediated depletion of Cep192 and Cep152. However, it fails to explain the striking differences in the precise centrosome localizations of Cep192, Cep152 and Plk4 and their cell cycle-regulation (Cizmecioglu et al., 2010; Sir et al., 2011; Sonnen et al., 2012; this study; Zhu et al., 2008). First, Cep192 levels at centrosomes increase drastically at the onset of mitosis (Gomez-Ferreria et al., 2007; Zhu et al., 2008; this study). This recruitment is not paralleled by an increase in total Cep192 protein level and thus likely governed by phosphorylation or other post-translational modifications. Considering that Plk1 has long been known to regulate centrosome maturation (Lane and Nigg, 1996) and that

Plk1 inhibition prevents Cep192 recruitment at the G2/M transition (Haren et al., 2009), it is intriguing that Cep192 is a likely physiological substrate of Plk1 (Santamaria et al., 2011). Second, Cep152 also undergoes cell cycle-regulated association with centrosomes and generally shows a more restricted localization than Cep192 (Cizmecioglu et al., 2010; Sonnen et al., 2012; this study). Third, Plk4 shows an even more restricted localization than either Cep192 or Cep152 (compare Sonnen et al., 2012 and Fig. 1 in this study). Collectively, these data indicate that complex formation between these proteins must be locally controlled throughout cell cycle progression. It is possible that Cep152 and/or Cep192 contribute to locally regulate Plk4 stability, as both Cep152 and Cep192 directly interact with Plk4 in in vitro binding assays. Conversely, Plk4 might regulate Cep152 and/or Cep192 through phosphorylation. It is also intriguing that Cep192 binds Aurora A (Joukov et al., 2010) and that both Cep152 and Cep192 harbor predicted docking sites for Plk1 (data not shown), strongly hinting at regulation by cell cycle kinases. Thus, multiple enzymes able to confer posttranslational modifications and/or as yet unidentified accessory factors are expected to cooperate in the spatiotemporal control of Cep192, Cep152 and Plk4. Understanding the detailed mechanisms that restrict the localization of Plk4 to the close proximity of pro-centriole formation (Sonnen et al., 2012) clearly represents a major challenge for future investigation.

Materials and Methods
Plasmids
Plasmids encoding Cep63 and Cep192-2 were kindly provided by F. Gergely (Cambridge, UK) (Sir et al., 2011) and D. J. Sharp (New York, USA) (Gomez-Ferreria et al., 2007), respectively. A Cep152-2 cDNA was obtained from Imagenes (clone IRCMp5012G0825D) and cloning of Plk4 and CPAP cDNAs was described previously (Habedanck et al., 2005; Schmidt et al., 2009). cDNA for Cep192-1 was obtained by amplifying the N-terminus of Cep192-1 (1–3986 bp) from a U2OS cDNA library and ligating the product into a construct containing Cep192-2 after restriction with KpnI: RNA was isolated from U2OS cells using the RNeasy Mini kit (QIAGEN) according to the manufacturer's instructions. RT-PCR was performed using Superscript III Reverse Transcriptase (Invitrogen) with oligo-dT primers (Invitrogen). Using the Polymerase Pfu Ultra II kit (Agilent Technologies) Cep192 cDNA was amplified with sequence-specific primers (Cep192-1-fw: TTTTGGCCGGCCAAATGGAAGATTTTCGAGGTA-TAGCAGAAGAATC and Cep192-1N-rv: CAGAGGGAAGAGGTACCCATCC-ATC). cDNAs were subcloned into pcDNA3.1 vectors providing N-terminal myc, or FLAG tags. GFP-tagged plasmids and the bacterial expression constructs for Cep192 and Plk4 were prepared via the Gateway technology (Invitrogen) using the pENTR/D-TOPO entry vector and pcDNA3.1(-)Puro/EGFP-C1, Nova pET-57-DEST (Novagen) or pDEST15 (Invitrogen), respectively.

Antibodies
Polyclonal rabbit antibodies against His-tagged Cep152 (aa1–87 and aa1378–1654) were raised at Charles River Laboratories (Elevages Scientifique des Dombes, Charles River Laboratories, Romans, France) and purified according to standard protocols (Sonnen et al., 2012). Monoclonal 9E10 anti-Myc (undiluted culture supernatant), monoclonal HE-12 anti-Cyclin E (undiluted culture supernatant), anti-Plk1, anti-Sas-6, polyclonal anti-Plk4 and anti-Cep135 (Kleylein-Sohn et al., 2007), anti-CP110 and anti-Cep192 (Schmidt et al., 2009), anti-Cep164 (Graser et al., 2007), anti-Cap350 (Yan et al., 2006) and monoclonal anti-Plk4 antibodies (Guderian et al., 2010) have been described previously. Antibodies against Cep63 (rabbit polyclonal), PCNA (mouse monoclonal) and glutamylated tubulin (GT335; mouse monoclonal) were kindly provided by F. Gergely (Cambridge, UK) (Sir et al., 2011), H. Leonhardt (Munich, Germany) and B. Eddé (Montpellier, France) (Wolff et al., 1992), respectively. A monoclonal antibody against Plk4, kindly provided by I. Hoffmann (Heidelberg, Germany) (Cizmecioglu et al., 2010) was used for detection of endogenous Plk4 by western blotting. Antibodies against NEDD1, α-tubulin, γ-tubulin, Pericentrin, cyclin B1 and FLAG were purchased from Sigma (Taufkirchen, Germany) and an antibody against GFP was purchased from Abcam. AlexaRed-594-, AlexaRed-555-, AlexaGreen-488-, AlexaCy5-647-labeled secondary anti-mouse and anti-rabbit antibodies were purchased from Invitrogen (Carlsbad, CA, USA) and CF405S-labeled secondary antibodies were purchased from Biotium. To simultaneously visualize different polyclonal rabbit antibodies, they were directly labeled with AlexaRed-594, AlexaRed-555, AlexaGreen-488 and AlexaCy5-647 fluorophores, using the corresponding Antibody Labeling Kits (Invitrogen). Whenever required, secondary antibodies were blocked using anti-FLAG antibodies prior to incubation with directly coupled antibodies of the same species.

Cell culture and transfections
All cells were grown at 37℃ in a 5% CO2 atmosphere. HeLa, U2OS or HEK293T cells were cultured in Dulbecco's modified Eagle's medium (DMEM), supplemented with 10% heat-inactivated fetal calf serum (FCS, PAN Biotech, Aidenbach, Germany) and penicillin-streptomycin (100 µg/ml, Gibco-BRL, Karlsruhe, Germany). The tetracycline-inducible U2OS myc-Plk4 WT cell line (U2OS:myc-Plk4) has been described previously (Kleylein-Sohn et al., 2007). U2OS:myc-Plk4 cells were cultured with 0.5 mg/ml G418 (Invitrogen) and 50 µg/ml hygromycin (Merck) and myc-Plk4 expression was induced by the addition of 1 µg/ml of tetracyclin. To induce S phase arrests, cells were incubated with either 1.6 µg/ml aphidicolin or 2 mM thymidine. For release cells were washed with PBS and incubated in culture medium. Transient transfections of HEK293T or U2OS cells with mammalian expression vectors or corresponding vector controls were performed using TransIT-LT1 transfection reagent (Mirus Bio, Madison, WI) according to the manufacturer's protocol.

siRNA-mediated protein depletion
Transfections were performed using Oligofectamin (Invitrogen) according to the manufacturer's protocol. The following siRNA duplex oligonucleotides were used: siGL2 CGTACGCGGAATACTTCGA (Elbashir et al., 2001), siCep152 #1 GCG-GATCCAACTGGAAATCTA (Graser et al., 2007), siCep152 #2 GCATT-GAGGTTGAGACTAA, siCep192 #1 AAGGAAGACATTTTCATCTCT (Zhu et al., 2008), siCep192 #2 CAGAGGAATCAATAATAAA (Gomez-Ferreria et al., 2007), siPlk4 CTGGTAGTACTAGTTCACCTA (Habedanck et al., 2005), siSas-6 CTAGATGATGCTACTAAGCAA (Graser et al., 2007), siPericentrin GCAGC-TGAGCTGAAGGAGA (Dammermann and Merdes, 2002), siCPAP GGAA-GATTGCACCAGTCAA (Schmidt et al., 2009), siCep63 CAACGCT-TGATTTATCAGCAA (Graser et al., 2007). Both siRNA oligonucleotides used for depletion of Cep152 or Cep192, respectively, gave similar results. Unless stated otherwise, results for Cep152 #1 and Cep192 #1 are shown. All siRNA duplex oligonucleotides were ordered from Qiagen, Hilden, Germany.

Cell extract preparation and biochemical assays
For immunoprecipitations, HEK293T cells were collected 24 hours after transfection, washed in PBS and lysed on ice for 30 minutes in lysis buffer [50 mM Tris-HCl pH 7.4, 0.5% IgePal, 150 mM NaCl, 50 mM NaF, 1 mM PMSF, 25 mM β-glycerophosphate, 1 mM vanadate, Complete Mini Protease Inhibitor Cocktail (Roche Diagnostics)]. Lysates were cleared by centrifugation for 15 minutes at 13,000 g, 4℃ and extracts incubated for 2 hours at 4℃ with proteinG beads (GE Healthcare) coated with 1 µg of antibodies, anti-FLAG M2 Affinity Gel (Sigma-Aldrich) or GFP-Trap agarose beads (ChromoTek). Immune-complexes bound to beads were washed three times with wash buffer (50 mM Tris-HCl pH 7.4, 1% IgePal, 300 mM NaCl). Bound proteins were eluted by boiling in 2× SDS sample buffer, resolved by SDS-PAGE and analyzed by western blotting.

Recombinant proteins were expressed by induction of BL21 DE3 E. coli with 1 mM IPTG for 18 hours at 16℃. Plk4 GST-fusion protein was purified using Glutathione Sepharose 4B beads (GE Healthcare); Cep192 fusion protein, harboring an N-terminal His- and NusA-tag and a C-terminal Strep-tag, was purified using Strep-Tactin Superflow beads (IBA GmbH, Germany) according to the manufacturer's instructions. GST-pulldown assays were performed by incubating proteins for 2 hours at 4℃ in 50 mM Tris-HCl pH 7.4, 0.5% IgePal, 150 mM NaCl, 1 mM DTT, 1 mM PMSF, Complete Mini Protease Inhibitor Cocktail (Roche Diagnostics), 2 µg/ml BSA, followed by incubation for 1 hour at 4℃ with Glutathione Sepharose 4B beads (GE Healthcare) and washing with wash buffer (50 mM Tris-HCL pH 7.4, 500 mM NaCl, 1% Igepal).

Microscopy
For fluorescence microscopy cells were grown on coverslips and fixed in methanol for 5 minutes at −20℃. Antibody incubations and washings were performed as described previously (Meraldi et al., 1999). Cells were analyzed using a DeltaVision microscope on a Nikon TE200 base (Applied Precision), equipped with an APOPLAN 100× 1.4 N.A. oil-immersion and a Plan Apochromat 60× 1.42 oil immersion objective (Olympus), and a CoolSNAP HQ2 camera (Photometrics). Serial optical sections obtained 0.2-µm apart along the z-axis were processed using a deconvolution algorithm and projected into one picture using Softworx. For quantitation of centrosomal protein levels with ImageJ, z-stacks were acquired with the same exposure and maximum-intensity projections were generated. Background signal intensity was subtracted from the centrosomal signal intensity.

3D-SIM was performed on a DeltaVision OMX-Blaze microscope system (version 4; Applied Precision, Issaquah, WA) equipped with 405, 445, 488, 514,

568 and 642 nm solid-state lasers. Images were acquired using a Plan Apo N 60× 1.42 NA oil immersion objective lens (Olympus) and four liquid-cooled sCMOs cameras (pco Edge, full frame 2560×2160; Photometrics). Exciting light was directed through a movable optical grating to generate a fine-striped interference pattern on the sample plane. The pattern was shifted laterally through five phases and three angular rotations of 60° for each z section. Optical z-sections were separated by 0.125 μm. The laser lines 488, 568 and 642 nm were used for 3D-SIM acquisition. Exposure times were typically between 10 and 250 milliseconds, and the power of each laser was adjusted to achieve optimal intensities of between 7000 and 10,000 counts in a raw image of 15-bit dynamic range at the lowest laser power possible to minimize photobleaching. Multichannel imaging was achieved through sequential acquisition of wavelengths by separate cameras. Raw 3D-SIM images were processed and reconstructed using the DeltaVision OMX SoftWoRx software package (Applied Precision; Gustafsson et al., 2008; Schermelleh et al., 2008). The resulting size of the reconstructed images was of 256×256 pixels. The channels were aligned in the image plane and around the optical axis using predetermined shifts as measured using a target lens and the SoftWoRx alignment tool. The channels were then carefully aligned using alignment parameter from control measurements with 1 μm diameter multi-spectral fluorescent beads (Invitrogen, Molecular Probes).

For electron microscopy, cells were grown on coverslips, fixed with 4% paraformaldehyde for 10 minutes, and permeabilized with PBS + 0.5% Triton X-100 for 2 minutes. Blocking in PBS + 2% BSA was performed for 30 minutes, primary antibody incubations were performed for 60 minutes and followed by incubation with goat-anti-mouse/rabbit IgG-Nanogold (1:50; Nanoprobes) for 50 minutes. Nanogold was silver-enhanced with HQ Silver (Nanoprobes). Cells were further processed as described previously (Fry et al., 1998).

Miscellaneous techniques

Protein alignments were performed using the software CLC Main Workbench 6.7.1. Data are represented as mean ± s.e.m. Pairwise comparisons were performed using Student's t-test. Significance is indicated as *$P<0.05$ and **$P<0.01$.

Author contributions

K.F.S. and E.A.N. conceived and designed the experiments. K.F.S., A.-M.G., E.A. and Y.-D.S. performed the experiments and analyzed the data. K.F.S. and E.A.N. wrote the manuscript.

Supplementary material available online at
http://jcs.biologists.org/lookup/suppl/doi:10.1242/jcs.129502/-/DC1

References

Azimzadeh, J., Wong, M. L., Downhour, D. M., Sánchez Alvarado, A. and Marshall, W. F. (2012). Centrosome loss in the evolution of planarians. *Science* **335**, 461-463.

Bahtz, R., Seidler, J., Arnold, M., Haselmann-Weiss, U., Antony, C., Lehmann, W. D. and Hoffmann, I. (2012). GCP6 is a substrate of Plk4 and required for centriole duplication. *J. Cell Sci.*. **125**, 486-496.

Basto, R., Brunk, K., Vinadogrova, T., Peel, N., Franz, A., Khodjakov, A. and Raff, J. W. (2008). Centrosome amplification can initiate tumorigenesis in flies. *Cell* **133**, 1032-1042.

Bettencourt-Dias, M., Rodrigues-Martins, A., Carpenter, L., Riparbelli, M., Lehmann, L., Gatt, M. K., Carmo, N., Balloux, F., Callaini, G. and Glover, D. M. (2005). SAK/PLK4 is required for centriole duplication and flagella development. *Curr. Biol.* **15**, 2199-2207.

Bettencourt-Dias, M., Hildebrandt, F., Pellman, D., Woods, G. and Godinho, S. A. (2011). Centrosomes and cilia in human disease. *Trends Genet.* **27**, 307-315.

Blachon, S., Gopalakrishnan, J., Omori, Y., Polyanovsky, A., Church, A., Nicastro, D., Malicki, J. and Avidor-Reiss, T. (2008). Drosophila asterless and vertebrate Cep152 Are orthologs essential for centriole duplication. *Genetics* **180**, 2081-2094.

Bonaccorsi, S., Giansanti, M. G. and Gatti, M. (1998). Spindle self-organization and cytokinesis during male meiosis in asterless mutants of Drosophila melanogaster. *J. Cell Biol.* **142**, 751-761.

Bornens, M. (2012). The centrosome in cells and organisms. *Science* **335**, 422-426.

Brownlee, C. W., Klebba, J. E., Buster, D. W. and Rogers, G. C. (2011). The Protein Phosphatase 2A regulatory subunit Twins stabilizes Plk4 to induce centriole amplification. *J. Cell Biol.* **195**, 231-243.

Carvalho-Santos, Z., Machado, P., Branco, P., Tavares-Cadete, F., Rodrigues-Martins, A., Pereira-Leal, J. B. and Bettencourt-Dias, M. (2010). Stepwise evolution of the centriole-assembly pathway. *J. Cell Sci.* **123**, 1414-1426.

Carvalho-Santos, Z., Azimzadeh, J., Pereira-Leal, J. B. and Bettencourt-Dias, M. (2011). Evolution: Tracing the origins of centrioles, cilia, and flagella. *J. Cell Biol.* **194**, 165-175.

Chang, J., Cizmecioglu, O., Hoffmann, I. and Rhee, K. (2010). PLK2 phosphorylation is critical for CPAP function in procentriole formation during the centrosome cycle. *EMBO J.* **29**, 2395-2406.

Cizmecioglu, O., Arnold, M., Bahtz, R., Settele, F., Ehret, L., Haselmann-Weiss, U., Antony, C. and Hoffmann, I. (2010). Cep152 acts as a scaffold for recruitment of Plk4 and CPAP to the centrosome. *J. Cell Biol.* **191**, 731-739.

Cunha-Ferreira, I., Rodrigues-Martins, A., Bento, I., Riparbelli, M., Zhang, W., Laue, E., Callaini, G., Glover, D. M. and Bettencourt-Dias, M. (2009). The SCF/Slimb ubiquitin ligase limits centrosome amplification through degradation of SAK/PLK4. *Curr. Biol.* **19**, 43-49.

Dammermann, A. and Merdes, A. (2002). Assembly of centrosomal proteins and microtubule organization depends on PCM-1. *J. Cell Biol.* **159**, 255-266.

Davis, E. E. and Katsanis, N. (2012). The ciliopathies: a transitional model into systems biology of human genetic disease. *Curr. Opin. Genet. Dev.* **22**, 290-303.

Delattre, M., Canard, C. and Gönczy, P. (2006). Sequential protein recruitment in C. elegans centriole formation. *Curr. Biol.* **16**, 1844-1849.

Dix, C. I. and Raff, J. W. (2007). Drosophila Spd-2 recruits PCM to the sperm centriole, but is dispensable for centriole duplication. *Curr. Biol.* **17**, 1759-1764.

Dobbelaere, J., Josué, F., Suijkerbuijk, S., Baum, B., Tapon, N. and Raff, J. (2008). A genome-wide RNAi screen to dissect centriole duplication and centrosome maturation in Drosophila. *PLoS Biol.* **6**, e224.

Dzhindzhev, N. S., Yu, Q. D., Weiskopf, K., Tzolovsky, G., Cunha-Ferreira, I., Riparbelli, M., Rodrigues-Martins, A., Bettencourt-Dias, M., Callaini, G. and Glover, D. M. (2010). Asterless is a scaffold for the onset of centriole assembly. *Nature* **467**, 714-718.

Elbashir, S. M., Harborth, J., Lendeckel, W., Yalcin, A., Weber, K. and Tuschl, T. (2001). Duplexes of 21-nucleotide RNAs mediate RNA interference in cultured mammalian cells. *Nature* **411**, 494-498.

Fode, C., Motro, B., Yousefi, S., Heffernan, M. and Dennis, J. W. (1994). Sak, a murine protein-serine/threonine kinase that is related to the Drosophila polo kinase and involved in cell proliferation. *Proc. Natl. Acad. Sci. USA* **91**, 6388-6392.

Fry, A. M., Meraldi, P. and Nigg, E. A. (1998). A centrosomal function for the human Nek2 protein kinase, a member of the NIMA family of cell cycle regulators. *EMBO J.* **17**, 470-481.

Ganem, N. J., Godinho, S. A. and Pellman, D. (2009). A mechanism linking extra centrosomes to chromosomal instability. *Nature* **460**, 278-282.

Gomez-Ferreria, M. A., Rath, U., Buster, D. W., Chanda, S. K., Caldwell, J. S., Rines, D. R. and Sharp, D. J. (2007). Human Cep192 is required for mitotic centrosome and spindle assembly. *Curr. Biol.* **17**, 1960-1966.

Gomez-Ferreria, M. A., Bashkurov, M., Mullin, M., Gingras, A. C. and Pelletier, L. (2012). CEP192 interacts physically and functionally with the K63-deubiquitinase CYLD to promote mitotic spindle assembly. *Cell Cycle* **11**, 3555-3558.

Gönczy, P. (2012). Towards a molecular architecture of centriole assembly. *Nat. Rev. Mol. Cell Biol.* **13**, 425-435.

Graser, S., Stierhof, Y. D., Lavoie, S. B., Gassner, O. S., Lamla, S., Le Clech, M. and Nigg, E. A. (2007). Cep164, a novel centriole appendage protein required for primary cilium formation. *J. Cell Biol.* **179**, 321-330.

Guderian, G., Westendorf, J., Uldschmid, A. and Nigg, E. A. (2010). Plk4 trans-autophosphorylation regulates centriole number by controlling betaTrCP-mediated degradation. *J. Cell Sci.* **123**, 2163-2169.

Guernsey, D. L., Jiang, H., Hussin, J., Arnold, M., Bouyakdan, K., Perry, S., Babineau-Sturk, T., Beis, J., Dumas, N., Evans, S. C. et al. (2010). Mutations in centrosomal protein CEP152 in primary microcephaly families linked to MCPH4. *Am. J. Hum. Genet.* **87**, 40-51.

Guichard, P., Desfosses, A., Maheshwari, A., Hachet, V., Dietrich, C., Brune, A., Ishikawa, T., Sachse, C. and Gönczy, P. (2012). Cartwheel architecture of Trichonympha basal body. *Science* **337**, 553.

Gustafsson, M. G., Shao, L., Carlton, P. M., Wang, C. J., Golubovskaya, I. N., Cande, W. Z., Agard, D. A. and Sedat, J. W. (2008). Three-dimensional resolution doubling in wide-field fluorescence microscopy by structured illumination. *Biophys. J.* **94**, 4957-4970.

Habedanck, R., Stierhof, Y. D., Wilkinson, C. J. and Nigg, E. A. (2005). The Polo kinase Plk4 functions in centriole duplication. *Nat. Cell Biol.* **7**, 1140-1146.

Haren, L., Stearns, T. and Luders, J. (2009). Plk1-dependent recruitment of gamma-tubulin complexes to mitotic centrosomes involves multiple PCM components. *PLoS One* **4**, e5976.

Hatch, E. M., Kulukian, A., Holland, A. J., Cleveland, D. W. and Stearns, T. (2010). Cep152 interacts with Plk4 and is required for centriole duplication. *J. Cell Biol.* **191**, 721-729.

Holland, A. J., Lan, W., Niessen, S., Hoover, H. and Cleveland, D. W. (2010). Polo-like kinase 4 kinase activity limits centrosome overduplication by autoregulating its own stability. *J. Cell Biol.* **188**, 191-198.

Holland, A. J., Fachinetti, D., Zhu, Q., Bauer, M., Verma, I. M., Nigg, E. A. and Cleveland, D. W. (2012). The autoregulated instability of Polo-like kinase 4 limits centrosome duplication to once per cell cycle. *Genes Dev.* **26**, 2684-2689.

Joukov, V., De Nicolo, A., Rodriguez, A., Walter, J. C. and Livingston, D. M. (2010). Centrosomal protein of 192 kDa (Cep192) promotes centrosome-driven spindle assembly by engaging in organelle-specific Aurora A activation. *Proc. Natl. Acad. Sci. USA* **107**, 21022-21027.

Kalay, E., Yigit, G., Aslan, Y., Brown, K. E., Pohl, E., Bicknell, L. S., Kayserili, H., Li, Y., Tüysüz, B., Nürnberg, G. et al. (2011). CEP152 is a genome maintenance protein disrupted in Seckel syndrome. *Nat. Genet.* **43**, 23-26.

Kemp, C. A., Kopish, K. R., Zipperlen, P., Ahringer, J. and O'Connell, K. F. (2004). Centrosome maturation and duplication in C. elegans require the coiled-coil protein SPD-2. *Dev. Cell* **6**, 511-523.

Kirkham, M., Müller-Reichert, T., Oegema, K., Grill, S. and Hyman, A. A. (2003). SAS-4 is a C. elegans centriolar protein that controls centrosome size. *Cell* **112**, 575-587.

Kitagawa, D., Busso, C., Flückiger, I. and Gönczy, P. (2009). Phosphorylation of SAS-6 by ZYG-1 is critical for centriole formation in C. elegans embryos. *Dev. Cell* **17**, 900-907.

Kitagawa, D., Vakonakis, I., Olieric, N., Hilbert, M., Keller, D., Olieric, V., Bortfeld, M., Erat, M. C., Flückiger, I., Gönczy, P. et al. (2011). Structural basis of the 9-fold symmetry of centrioles. *Cell* **144**, 364-375.

Kleylein-Sohn, J., Westendorf, J., Le Clech, M., Habedanck, R., Stierhof, Y.-D. and Nigg, E. A. (2007). Plk4-induced centriole biogenesis in human cells. *Dev. Cell* **13**, 190-202.

Lane, H. A. and Nigg, E. A. (1996). Antibody microinjection reveals an essential role for human polo-like kinase 1 (Plk1) in the functional maturation of mitotic centrosomes. *J. Cell Biol.* **135**, 1701-1713.

Leidel, S. and Gönczy, P. (2003). SAS-4 is essential for centrosome duplication in C elegans and is recruited to daughter centrioles once per cell cycle. *Dev. Cell* **4**, 431-439.

Leidel, S., Delattre, M., Cerutti, L., Baumer, K. and Gönczy, P. (2005). SAS-6 defines a protein family required for centrosome duplication in C. elegans and in human cells. *Nat. Cell Biol.* **7**, 115-125.

Lüders, J. and Stearns, T. (2007). Microtubule-organizing centres: a re-evaluation. *Nat. Rev. Mol. Cell Biol.* **8**, 161-167.

Lukinavičius, G., Lavogina, D., Orpinell, M., Umezawa, K., Reymond, L., Garin, N., Gönczy, P. and Johnsson, K. (2013). Selective chemical crosslinking reveals a Cep57-Cep63-Cep152 centrosomal complex. *Curr. Biol.* **23**, 265-270.

Megraw, T. L., Sharkey, J. T. and Nowakowski, R. S. (2011). Cdk5rap2 exposes the centrosomal root of microcephaly syndromes. *Trends Cell Biol.* **21**, 470-480.

Meraldi, P., Lukas, J., Fry, A. M., Bartek, J. and Nigg, E. A. (1999). Centrosome duplication in mammalian somatic cells requires E2F and Cdk2-cyclin A. *Nat. Cell Biol.* **1**, 88-93.

Nigg, E. A. (2002). Centrosome aberrations: cause or consequence of cancer progression? *Nat. Rev. Cancer* **2**, 815-825.

Nigg, E. A. (2007). Centrosome duplication: of rules and licenses. *Trends Cell Biol.* **17**, 215-221.

Nigg, E. A. and Raff, J. W. (2009). Centrioles, centrosomes, and cilia in health and disease. *Cell* **139**, 663-678.

O'Connell, K. F., Maxwell, K. N. and White, J. G. (2000). The spd-2 gene is required for polarization of the anteroposterior axis and formation of the sperm asters in the Caenorhabditis elegans zygote. *Dev. Biol.* **222**, 55-70.

O'Connell, K. F., Caron, C., Kopish, K. R., Hurd, D. D., Kemphues, K. J., Li, Y. and White, J. G. (2001). The C. elegans zyg-1 gene encodes a regulator of centrosome duplication with distinct maternal and paternal roles in the embryo. *Cell* **105**, 547-558.

Pelletier, L., Ozlü, N., Hannak, E., Cowan, C., Habermann, B., Ruer, M., Müller-Reichert, T. and Hyman, A. A. (2004). The Caenorhabditis elegans centrosomal protein SPD-2 is required for both pericentriolar material recruitment and centriole duplication. *Curr. Biol.* **14**, 863-873.

Pelletier, L., O'Toole, E., Schwager, A., Hyman, A. A. and Müller-Reichert, T. (2006). Centriole assembly in Caenorhabditis elegans. *Nature* **444**, 619-623.

Puklowski, A., Homsi, Y., Keller, D., May, M., Chauhan, S., Kossatz, U., Grünwald, V., Kubicka, S., Pich, A., Manns, M. P. et al. (2011). The SCF-FBXW5 E3-ubiquitin ligase is regulated by PLK4 and targets HsSAS-6 to control centrosome duplication. *Nat. Cell Biol.* **13**, 1004-1009.

Rodrigues-Martins, A., Riparbelli, M., Callaini, G., Glover, D. M. and Bettencourt-Dias, M. (2007). Revisiting the role of the mother centriole in centriole biogenesis. *Science* **316**, 1046-1050.

Rogers, G. C., Rusan, N. M., Roberts, D. M., Peifer, M. and Rogers, S. L. (2009). The SCF Slimb ubiquitin ligase regulates Plk4/Sak levels to block centriole reduplication. *J. Cell Biol.* **184**, 225-239.

Santamaria, A., Wang, B., Elowe, S., Malik, R., Zhang, F., Bauer, M., Schmidt, A., Sillje, H. H., Korner, R. and Nigg, E. A. (2011). The Plk1-dependent phosphoproteome of the early mitotic spindle. *Mol. Cell. Proteomics* **10**, M110.004457.

Schermelleh, L., Carlton, P. M., Haase, S., Shao, L., Winoto, L., Kner, P., Burke, B., Cardoso, M. C., Agard, D. A., Gustafsson, M. G. et al. (2008). Subdiffraction multicolor imaging of the nuclear periphery with 3D structured illumination microscopy. *Science* **320**, 1332-1336.

Schmidt, T. I., Kleylein-Sohn, J., Westendorf, J., Le Clech, M., Lavoie, S. B., Stierhof, Y. D. and Nigg, E. A. (2009). Control of Centriole Length by CPAP and CP110. *Curr. Biol.* **19**, 1005-1011.

Sillibourne, J. E., Tack, F., Vloemans, N., Boeckx, A., Thambirajah, S., Bonnet, P., Ramaekers, F. C., Bornens, M. and Grand-Perret, T. (2010). Autophosphorylation of polo-like kinase 4 and its role in centriole duplication. *Mol. Biol. Cell* **21**, 547-561.

Sir, J. H., Barr, A. R., Nicholas, A. K., Carvalho, O. P., Khurshid, M., Sossick, A., Reichelt, S., D'Santos, C., Woods, C. G. and Gergely, F. (2011). A primary microcephaly protein complex forms a ring around parental centrioles. *Nat. Genet.* **43**, 1147-1153.

Slevin, L. K., Nye, J., Pinkerton, D. C., Buster, D. W., Rogers, G. C. and Slep, K. C. (2012). The structure of the plk4 cryptic polo box reveals two tandem polo boxes required for centriole duplication. *Structure* **20**, 1905-1917.

Song, M. H., Liu, Y., Anderson, D. E., Jahng, W. J. and O'Connell, K. F. (2011). Protein phosphatase 2A-SUR-6/B55 regulates centriole duplication in C. elegans by controlling the levels of centriole assembly factors. *Dev. Cell* **20**, 563-571.

Sonnen, K. F., Schermelleh, L., Leonhardt, H. and Nigg, E. A. (2012). 3D-structured illumination microscopy provides novel insight into architecture of human centrosomes. *Biol. Open* **1**, 965-976.

Strnad, P. and Gönczy, P. (2008). Mechanisms of procentriole formation. *Trends Cell Biol.* **18**, 389-396.

Thornton, G. K. and Woods, C. G. (2009). Primary microcephaly: do all roads lead to Rome? *Trends Genet.* **25**, 501-510.

van Breugel, M., Hirono, M., Andreeva, A., Yanagisawa, H. A., Yamaguchi, S., Nakazawa, Y., Morgner, N., Petrovich, M., Ebong, I. O., Robinson, C. V. et al. (2011). Structures of SAS-6 suggest its organization in centrioles. *Science* **331**, 1196-1199.

Varmark, H., Llamazares, S., Rebollo, E., Lange, B., Reina, J., Schwarz, H. and Gonzalez, C. (2007). Asterless is a centriolar protein required for centrosome function and embryo development in Drosophila. *Curr. Biol.* **17**, 1735-1745.

Wolff, A., de Néchaud, B., Chillet, D., Mazarguil, H., Desbruyères, E., Audebert, S., Eddé, B., Gros, F. and Denoulet, P. (1992). Distribution of glutamylated alpha and beta-tubulin in mouse tissues using a specific monoclonal antibody, GT335. *Eur. J. Cell Biol.* **59**, 425-432.

Yan, X., Habedanck, R. and Nigg, E. A. (2006). A complex of two centrosomal proteins, CAP350 and FOP, cooperates with EB1 in microtubule anchoring. *Mol. Biol. Cell* **17**, 634-644.

Zhu, F., Lawo, S., Bird, A., Pinchev, D., Ralph, A., Richter, C., Müller-Reichert, T., Kittler, R., Hyman, A. A. and Pelletier, L. (2008). The mammalian SPD-2 ortholog Cep192 regulates centrosome biogenesis. *Curr. Biol.* **18**, 136-141.

Supplemental Material

- **Supplementary Figure 1**: Isoforms of Cep152
- **Supplementary Figure 2**: Isoforms of Cep192 – identification of N-terminal extension

(Supplementary Figures 1 and 2 provide analyses of potential Cep152 and Cep192 isoforms including their expression in selected human cell lines.)

- **Supplementary Figure 3**: Cell cycle-dependent centrosome localization of Cep152 and Cep192.

(Supplementary Figure 3 shows a side-by-side comparison of cell cycle-dependent localizations and cellular protein levels of Cep152 and Cep192, related to Figure 1.)

- **Supplementary Figure 4**: Dependency of centriolar localization of Cep63 on Cep152 and Cep192.

(Supplementary Figure 4 provides another example for the dependency of centriolar proteins on Cep152 and Cep192.)

- **Supplementary Figure 5**: Cep152 and Cep192 co-operate to recruit Plk4 to centrosomes.

(In Supplementary Figure 5 Pericentrin depletion is shown as a negative control for the role of Cep192 and Cep152 in the centrosome recruitment of Plk4. In addition co-operation of Cep192 and Cep152 in centriolar recruitment of newly synthesized Plk4 is illustrated.)

- **Supplementary Figure 6:** Cep152 and Cep192 interact with Plk4 through similar acidic patches within their Plk4-binding domains.

(Supplementary Figure 6 shows the mapping of the Plk4-binding domain within Cep152 as well as alignments of Plk4-binding domains shared between Cep152 and Cep192 homologs, illustrating evolutionary conservation of acidic stretches.)

Supplementary Figure 1

Isoforms of Cep152.

A. Four potential Cep152 isoforms, termed Cep152-1 to Cep152-4, are generated by alternative splicing. They are illustrated schematically, together with their predicted molecular weights (MW) and lengths in amino acids (AA). Based on the presence of an extended C-terminus long (Cep152-1 and/or -2) and short forms of Cep152 (Cep152-3 and/or -4) can be distinguished. Two antibodies, Cep152-N and Cep152-C, were raised against the indicated regions. Databases provide full length transcript support for human Cep152-1, Cep152-2 and Cep152-3 (BX648822.1, BC117182.1, AB020719.1); using primers specific for the long Cep152 isoforms Cep152-2 was amplified from a HeLa cDNA library (data not shown).

B. HEK293T cells were transfected with the indicated plasmids and lysates were analysed by SDS PAGE and Western Blotting (WB), using antibodies against Flag, Cep152-N, Cep152-C and α-Tubulin. Note that Cep152-C recognizes only the isoform Cep152-2, whereas Cep152-N recognizes both Cep152-2 and Cep152-4. The asterisk denotes a non-specific band.

C. HEK293T cells were transfected with the indicated plasmids for 18 h. After lysis immunoprecipitations were performed using Cep152-N and Cep152-C antibodies and rabbit IgG as control. Immunoprecipitates were analyzed by Western Blotting (WB) using the indicated antibodies. Note that Cep152-N immunoprecipitates all versions of Cep152 analyzed, whereas Cep152-C precipitates only the version with the extended C terminus, i.e. full length Cep152-2.

D. HeLa S3 and U2OS were transfected with the indicated siRNA oligonucleotides for 48 h. After lysis the samples were analyzed by Western Blotting (WB) using the indicated antibodies.

Supplementary Figure 2

Isoforms of Cep192: identification of N-terminal extension.

A. Four Cep192 isoforms generated by alternative splicing are potentially expressed in human cells. These were termed Cep192-1 to Cep192-4. The isoforms together with their predicted molecular weights (MW) and lengths in amino acids (AA) are illustrated schematically. Also shown is the region against which the Cep192 antibody was generated. Green colouring illustrates alternative translation start sites.

B. HeLa S3 and U2OS cells were transfected with the indicated siRNA oligonucleotides for 72 h. After lysis the samples were analysed by Western Blotting (WB). α-Tubulin was analysed for loading control. Note that a prominent band above 250 kDa was strongly diminished upon depletion of Cep192 from both cell lysates.

Supplementary Figure 3

Cell cycle-dependent centrosome localization of Cep152 and Cep192.

A. U2OS cells were fixed and stained with the indicated antibodies. DAPI was used to visualize DNA. Cells harbouring centrioles before and after duplication were identified based on the number of CP110 dots. In the upper panel representative images are shown. Scale bar represents 1 μm (5 μm in the overview images to the right). In the lower panel Cep152 levels at Cep164-positive and Cep164-negative centrioles are quantified (15 cells, error bars denote standard deviation).

B. HeLa S3 cells were released from a double thymidine arrest and samples taken every two hours. After lysis the samples were analyzed by Western Blotting using the indicated antibodies.

C,D. U2OS cells were fixed and stained with the indicated antibodies. DNA was stained with DAPI. Different cell cycle stages were identified based on the number of CP110 dots per cell as well as the morphology of DNA staining. Representative images for Cep152 localization (**C**) and Cep192 localization (**D**) are shown. Scale bars represent 1 μm (5 μm in the overview images to the right).

E. U2OS cells were transfected for 48 h with Flag-Cep192-1 or Flag-Cep192-2 plasmids or vector control. After fixation cells were stained with the indicated antibodies and analysed by immunofluorescence microscopy. DAPI was used to visualize DNA. Scale bars represent 1 μm (5 μm in the overviews to the right).

Supplementary Figure 4

Dependency of centriolar localization of Cep63 on Cep152 and Cep192.

To investigate the dependency of Cep63 localization on Cep152 (**A**) and Cep192 (**B**), U2OS cells were transfected with the indicated siRNA oligonucleotides for 72 h. After fixation the cells were stained with the indicated antibodies. PCNA was used identify cells in S phase. Scale bars represent 1 μm (5 μm in the overview images to the right).

Supplementary Figure 5

Cep192 and Cep152 co-operate to recruit Plk4 to centrosomes.

A. Pericentrin depletion does not impair recruitment of Plk4 to centrosomes. U2OS cells were transfected with the indicated siRNA oligonucleotides for 72 h. After fixation the cells were stained with the indicated antibodies and analyzed by immunofluorescence microscopy. Anti-PCNA antibodies were used to visualize cells in S phase. Scale bars 1 μm or 5 μm (overview images).

B. Cep152 and Cep192 co-operate in recruitment of over-expressed Plk4 to centrosomes. U2OS:myc-Plk4 cells were transfected with the indicated siRNA oligonucleotides for 48 h and then myc-Plk4 expression was induced for 16 h. After fixation the cells were stained with the indicated antibodies for immunofluorescence microscopy. DNA was stained with DAPI. Fluorescence intensities were not quantified due to considerable variations of Plk4 expression within a cell population. Scale bars represent 1 μm or 5 μm (overview images, right panels).

Supplementary Figure 6

Conserved acidic patches within Cep152 and Cep192 are required for interaction with Plk4.

A. Cep152 residues 1 – 46 are sufficient for interaction with Plk4 (region corresponds to conserved region CR1 identified by Hatch et al. [1]). HEK293T cells were transfected with the indicated plasmids for 18 h. Lysates were subjected to anti-GFP immunoprecipitations and analyzed by Western blotting (WB).

B,C. Alignments of Plk4 interaction domains within Cep192 (**B**) and Cep152 (**C**) homologs from different species. Yellow shading indicates Plk4 binding domains mapped in this study for the human proteins. Amino acid residues are color-coded: red = acidic, blue = basic, green = polar, black = non-polar).

A G1 Phase / S/G2 Phase panels: Cep152-N, CP110, Cep164, Merge, Merge + DAPI. Bar graph: a. u. Cep152 vs CP110 Dots (2, 4) with Cep164 (+/−).

B Western blots: asyn, h after Thymidine Release (0 2 4 6 8 10 12 14). Cep152 long / Cep152 short (Shorter Exposure, Longer Exposure), Cep152-N; Cep192-1; Cyclin E; Cyclin B; Plk1; α-Tubulin.

C Cep152-N, CP110, Cep164, Merge, Merge + DAPI — Prophase, Metaphase, Anaphase, Telophase.

D Cep192, CP110, Cep164, Merge, Merge + DAPI — Prophase, Metaphase, Anaphase, Telophase.

E Interphase / Mitosis: Flag, CP110, Cep135, Merge, Merge + DAPI — Vector Control, Flag-Cep192-1, Flag-Cep192-2.

A

	Cep152-N	Cep63	Cep135	Merge	Merge + PCNA
siGL2					
siCep63					
siCep152					

B

	Cep192	Cep63	Cep135	Merge	Merge + PCNA
siGL2					
siCep63					
siCep192					

A Western blot panels: Input and IP: GFP, both GFP-Cep152 (GFP, 1-220, 1-46, 46-220) + myc-Plk4; WB: anti-GFP and WB: anti-myc.

B Sequence alignment

```
Homo sapiens         PRERLQLSFQ DDDSISRK-- KSYVESQRLS NALSKQSALQ METAGPEEEP AGATESLQGQ DLFNRASPLE QAQDSPID-F HLQSWMNNKE  171
Equus caballus       PREKLQLSFQ DDDSMSKK-- KNYMESQHLS DAVLKELAFQ RDTARTEEEQ TKTAKSFQSQ DLFGRISPLE QMQDSPVD-F CLPSWMNDKD  171
Mus musculus         PRERLRLSFQ GDDSALRK-- KNYIESPDLS HALMKPRA-- ------EEKQ ANAA-SVQGQ SLLGGVSPLQ QVPDSALD-F HLKSWTNHEE  163
Gallus gallus        PMGRFAISFR DDMEVATQ-- SKEPQPTVVS ---------- -------LKE SYSVPGDQGQ NVIERSN--- RSQDTLLEVY HLNDW-----  148
Xenopus laevis       AQRKFMLSFK DELEPFSNII GNQNQTVKLS ESDRKEKRSS DSEDPHKKRD SSSTCTLPRT KQIGKASKLT NANLNAMK--  ----------  161
Danio rerio          -KEKIALSLK EDLDSIDEFI AANRFSDLLV NV-------- ------NFD ETESAAFTKS SSSGGAVPLL VSNSVPLRTT DKDTMAAEAT  138
Drosophila melanogaster ----QMRLS-- ---------- --TNIS ELV------- ---------- ---------- TDDTIDLNSS SSFALVTPAT KGTNISFEPA EITG------  129
```

```
                              190                                                                     240
Homo sapiens         PKIVVLDAGK HFEDKTLKSD ---LSHTSLL ENEKLILPTS LED-SSDDDI DDEMFYDDHL EAYFEQLAIP GMIYEDLEGP EPPEKGFKLP  257
Equus caballus       NKIVIPDDGK HFEDKNPNND ---LSHTSLI ENEKLMSLTS LEG-SSDDDI DDEEFYDDHL EAYFEQLAIP GMIYEDLEGQ EPPEKDFKLS  257
Mus musculus         HNIAMPDPKK HFEAVNPNRD ---FSHTSLL DNEKLLTLTN LDS-SSDDDI NDEEFYDDHL EAYFEQLAIP GMMYE-AGGQ ESPADDFKFP  248
Gallus gallus        -KVTPSEPSE KLVETETSSD HLSISLSSFL ENEKLSSLSS LGGDSTDDDI DDEEFFDNQL EAYFEQLIPP DMN----RGD TDIGKLSKCC  233
Xenopus laevis       ---------- ---ENEDLFKD DLSKSVTSFL ENEKLLSIAS LEG-SSSDDL DDEEFYDDHL EAYFKKLLPH GMQRGVIEGQ EITEPKRLSH  238
Danio rerio          VFQVILEEE- --DGEETDSE KCSDSFSSFL ANEKLMSLDS MNSDMTDDDI DVTQLHDEEL ELYFNKLIPP AMQRGRVEGQ EISVELPSSS  225
Drosophila melanogaster -RSTLCQAGK QRRREKPSLS VAEILKSSFV EKARLL---- ---------- --ERKLQDAS QA--------  ----------  ----------  174
```

C Sequence alignment

```
                    1                                                          46
Homo sapiens         M-----SLDF GSVALPV-- --QNEDEEYD EEDYEREKEL QQLLTDLPHD MLDD--DLSS PEL-QYSDCS EDGTDGQPHH PEQLEMSWN-  76
Equus caballus       M-----SLDF GSVALQT-- --QNEDEEYD KEDYEREKEL QQLLTDLPHD MLDD--DLSS PEL-HSLDCS EDGIEGEPHR SDQSEMNWNV  77
Mus musculus         M-----SLEF GSVALQT-- --QNEDEEFD KEDFEREKEL QQLLTDLPHD MLDD--ELSS PER-HDSDCS MDGRAAEPHP SEHLERKWIE  77
Gallus gallus        M-----SLDF DSGALQT--- --QHEDEDYD QEDYAREQEL QQLLTDLPHD MLED----SG DQLSNYSDSS IHETEEQSGE ARKPDGRWND  76
Xenopus laevis       M-----SIDF DSGALQT--- --QQEEEYD KEDYAREQEL QQLLTDLPHD MLDD--SLSS PEPSYSDCS GHEISEKIPQ WEH-GANWGN  77
Danio rerio          M-----SLDF DSAALQT--- --QRQEEEYD QEDYAREQEL HKLLTDLPDD MLDDSADCSS PEL-NHSTCS HPEDNNRPQQ AWNNVP-QWEH  78
Drosophila melanogaster MNTPGISLFQ GADALNINST LDRQEEEEAL QDQKRREEEL GRIMVNAFDD LLDEENTIDS ---------- ---------- TTNYQSELEQ  70
```

```
Homo sapiens         EQMLPKSQS- -V------NGY NEIQ---SLY AG-------- ---EKCGNVW EENRSKTEDR HP-------- VYHP--EEGG DE---GGSGY  132
Equus caballus       HRVLPKSXX- -X-------- ---------- ---------- ---------- ---------- ---------- ---------- ----------  87
Mus musculus         RDILPKPHS- -M-------N- ---------- ---------- ---CGNGW EENRSKTEDQ HL-------- GYHP--GEGG DE---GGSGY  120
Gallus gallus        HLLI---NDA- -Q------NGY EQGQ----NLY PDQFLCDQQN DHVEKHAKNW NGLHSSEQMK HLYDVKEDYS GQNS---QEDP DDIYLDRDGF  152
Xenopus laevis       DD-LPNHQKP YK------NGF TENQYCMGFV GKQDEHLRNQ AGRDKMSNGW DVLHANEDDP -MFNGKYRYS KDHAYNSESN GQAFHGGDHY  160
Danio rerio          SR--PSHEEH YEEYAEGSYH EDYSYRSHTS QANTHPHHLQ PGTENAPSAW --------DP HNDQSYQYHS GDYAHSSAGT D-----GSHA  153
Drosophila melanogaster PPVLPNYPS- ---------- ---------- ---------- ---------- ---------- --HPH----- ---------- ----------  82
```